October 2007 Volume 2 Issue 3

Physical CHEMISTRY
An Indian Journal

Trade Science Inc.

Full Paper

PCAIJ, 2(3), 2007 [187-191]

# P-Type$(Bi_{0.25}\ Sb_{0.75})_2Te_3$ Thermoelectric Element Fabrication And Characterization

**Ghassem Kavei**

**Material and Energy Research Center(MERC), Tehran-14155-4777,(IRAN)**

*Received: 4th August, 2007 ; Accepted: 9th August, 2007*

## ABSTRACT

$Bi_2Te_3$ based solid solutions, are widely utilized as thermoelectric(TE) materials in peltier modules, in order to attain higher figure of merit(Z) a fraction of weight at different percentage of Sb is added. The compound Bi-Te-Sb prepared by unidirectional solidification techniques such as melting accompanied with oscillating the melted compound followed by, crystallizing by zone growth method. This work is focused on, the preparation and characterization of the samples with formula $Bi_2Te_3$ and$(Bi_{0.25}\ Sb_{0.75})_2\ Te_3$.$(Bi_{0.25}\ Sb_{0.75})_2\ Te_3$ are known as p-type TE pellet, this compound has a higher Z compared with other solid solutions of the Sb-Bi , which have been tested as p-type pellet. The major aspects of TE such as electrical and thermal conductivities and seebeck coefficient, which directly affect the figure of merit were measured. X-ray powder diffraction analysis of$(Bi_{0.25}\ Sb_{0.75})_2\ Te_3$ compared with $Bi_2Te_3$ suggests that the grown crystals are stoichiometric for$(Bi_{0.25}\ Sb_{0.75})_2\ Te_3$. It should also be noted that there is a strong relation between Z, balancing charge carriers and phonons of the compound, but they will not be discussed here. From experimental results $Z\approx2.7\times10^{-3}K^{-1}$ was obtained, this is the same value which was reported in the previous work.



## KEYWORDS

Narrow band gap;
Rhombohedral structure;
Stoichiometric solution;
Isomorphous crystallization;
Anisotropic semiconductor.

## INTRODUCTION

Bismuth telluride compounds are of great interest due to their high potential for technological applications. These compounds are widely used in many fields such as power supply and refrigeration due to their ability to produce significant temperature gradient with the application of current. $Bi_2Te_3$ compounds are layered crystals having rhombohedral unit cell and symmetry space group of $D^5$3d(R.3-m), with two-and three fold axes of symmetry $C_2$ and $C_3$, respectively[1]. It belongs to the narrow band gap semiconductor($E_g$=0.15eV) and finds a few applications in temperature control of laser diodes[2], optical recording system and strain gauges[3].

Bismuth is a semimetal, its crystal structure is based on rhombohedral lattice, with only slight distortion from fcc structure. The semi metallic properties of Bismuth are the result of slightly overlapping electron and hole bands. The Brillouin zone(Bz) of Bi is nearly identical to that of fcc structure cubic lattice. Hence the various

Full Paper

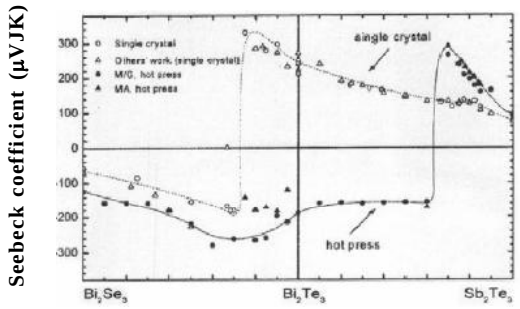


**Figure1 : Isomorphous$(Bi_{1-x}Sb_x)_2Te_3$ , with x≥0.75, Antimony reached solid solutions(p-type), and Bismuth reached solid solutions with x≥0.75(n-type) crystallize in the rhombohedral structure[6]**

symmetry points can be labeled in the same manner as those in the Bz of the fcc lattice. However, the distortion from the cubic lattice causes the L points to be centered in pseudo- square faces. The Γ points remain in the center of hexagonal faces.

Proposition for Bi remain valid for $Bi_{1-x}Sb_x$ for $0 \le x \le 0.15$. In support of this view Brant et.al[4] have shown that the electron Fermi energy surface decrease in volume with increasing Sb concentration, but remain geometrically unchanged within 9-10%.

Pure Bismuth and pure Antimony are semimetals, as are $Bi_{1-x}Sb_x$ alloys with x a few atomic percent at low temperature near 0 K,[5]. The experimental information on Bi-Sb with x at the above mentioned range show semiconductor properties.

$(Bi_{1-x}Sb_x)_2Te_3$ solid solutions consisting of isomorphous $Sb_2Te_3$ and $Bi_2Te_3$, with x≥0.75, Antimony reached solid solutions(p-type), and Bismuth reached solid solutions with x≤0.75(n-type) crystallize in the isomorphous solid solutions(see figure 1[6],). Bi atoms are substituted by Sb atoms. Volotskii and Syidnev[7] have reported a band structure with two-band model for both conduction and valence bands of the solid solutions. The calculation of band edge parameters of Bismuth and $Bi_{1-x}Sb_x$ alloys with $0 \le x \le 0.15$ have been presented by[5].

Okhotin et a.l[8], have studied the variation of thermal conductivity, electrical conductivity and seebeck coefficient of the materials in different categories. Metals are poor TE materials with a low seebeck coefficient and they have large electronic contribution to thermal conductivity with respect to semiconductors or insulators, so σ and κ will cancel each other. Insulators have a high Seebeck coefficient, and a small electronic contribution to thermal conductivity, but their charge density and therefore electrical conductivity are low leading to a low TE effect. The best TE materials are those between metals and insulators; i.e. semiconductors with an electronic charge density of $10^{19}cm^{-3}$[8]. The electrical properties of semiconducting materials can change dramatically with temperature. It is therefore, semiconductors can only function as TE materials over certain temperature ranges, which will vary for each semiconductor[9].

Nolas and Slack[10] have considered the effectiveness of most commonly used semiconductor materials for TE devices. It is therefore, known TE materials fall into three categories depending on their temperature range of operation. Bismuth telluride and its alloys have the highest ZT, and are extensively employed in terrestrial cooling. The most commonly used semiconductor material for cooling applications, bismuth telluride system($Bi_2Te_3$), has a maximum performance at approximately 350K with an effective operating range(EOR) of 170K to 470K. Bi-Sb alloys are useful only at low temperatures. Lead Telluride(PbTe), the next most commonly used material, is typically used for power generation but is not as efficient as $Bi_2Te_3$ in cooling applications. PbTe reaches a peak ZT at 620K and has an EOR of 573 to 773K.$(TeGe)_{1-x}(AgSbTe)_x$, alloys(TAGS), where x ~0.2, and has an EOR of 673-873K. SiGe, has an EOR of 1073-1273K and has been widely used in TE generators for space applications together with TAGS. The skutterudite, $CeFe_3CoSb_{12}$, has an EOR of 673 to 973K but is not used in practice since TAGS is superior in the same temperature range.

A TE couple/module consists of n- and p-type TE materials, where n and p stands for the negative and positive types of charge carriers within the material, respectively. The working principle of a typical TE couple is, as the electrons move from the p-type material to the n-type material through an electrical connector, the electrons jump to a higher energy state absorbing thermal energy(cold side). Continuing through the lattice of material, the electrons flow from the n-type material to the p-type material through an electrical connector, dropping to a lower energy state and releasing energy as heat to the heat sink(hot side).

A TE converter module consists of a number of alternate ingot-shaped n-and p-type semiconductor thermo elements, which are connected electrically in series with

metal connecting strips, sandwiched between two electrically insulating but thermally conducting ceramic plates(e.g., AlN). When an electric current is passed through the module, heat is absorbed at one face of the module and rejected at the other face hence the device works as a refrigerator[11]. The efficiency of the device is usually given as a percentage of carnot efficiency. Present TE devices operate at about 10% of carnot efficiency while the efficiency of compressors is about 30% and increases with size. There is no known limit for the efficiency of TE device, except for the carnot limit[12].

TE properties of anisotropic semiconductor, electronic structure and its relation to TE properties of $Bi_2Te_3$ were studied by several authors[13-15]. It is a common practice to fabricate $Bi_2Te_3$-based TE materials by means of crystal growth[16-17] and other methods[18-22]. In this work, a novel crystal growth process was developed to fabricate $Bi_2Te_3$-based TE materials. It is possible to obtain a high figure of merit due to careful crystallization and annealing ingots. XRD spectra confirm this state. We have fabricated p-type$(Bi_{1-x}Sb_x)_2Te_3$ crystallized ingots, compared with $Bi_2Te_3$ XRD spectra and then measured their TE parameters, i.e. electrical conductivity $\sigma$, thermal conductivity $\kappa$ and Seebeck coefficient $\alpha$. We have defined the figure of merit from a formula, $Z=\alpha^2\sigma/K$ which quoted in the enormous papers and texts.

## EXPERIMENTAL

To fabricate p-type$(Bi_{1-x}Sb_x)_2Te_3$ compound with x=0.75, the elements of Bi, Te and Sb were purified up to 5N purity. The powder mixtures were placed into a quartz tube, and the tube is evacuated below $10^{-5}$ Torr and the tube was heated to $250^0$C for degassing from wall of the cylindrical furnace. Then the Nitrogen or Argon gas was admitted into the vacuum system to remove the reacting atmospheric gases such as hydrogen and oxygen. This procedure secured the undesired reactions of the gases with the elements not to be occurred, when the sintering was carried out. The evacuated tubes were at $10^{-4}$ Torr and sealed. The powder mixture was sintered at $700^0$C to obtain a melt. The melt in the tube was stirred with 80 oscillations per minute at $700^0$C, for one hour using a rocking furnace to make a homogeneous melt without segregation. The tube containing the melt was quenched at a $200^0$C oil tank, and then cooled to room temperature. The solidified ingot was pulverized and filled in a quartz tube(~300mm length and 8mm diameter). The inside wall of the tube was carbon coated by acetone cracking to prevent adhesion of the compounds and Te diffusion deep into the tube wall. According to above-mentioned process, the tube was evacuated again to $10^{-4}$ Torr and sealed. The tube was placed in a vertical melting-zone system to crystallize the material at a speed of 13mm.$h^{-1}$. The crystallized ingot in the tube was annealed at $300^0$C for 24h, then cooled down to room temperature for 5h. The ingot was taken off the tube ready to characterize. In order to provide a good conductive surface, a solution of $HNO_3$ : $H_2O$=1:5 was used in etching and cleaning of the ingot surface.

The microstructural properties of the sample were investigated by X-ray diffraction(XRD). The conventional X-ray diffractometer with a target of $Cu_{K\alpha}$($\lambda$=1.54056Å)

**TABLE 1: The data for the $Bi_2Te_3$, $Sb_2Te_3$, $Sb_{0.405}Te_{0.595}$ and$(Bi_2Te_3)_{0.25}(Sb_2Te_3)_{0.75}$ structures**

| $Bi_2Te_3$ | | | | | | $Sb_{0.405}Te_{0.595}$ | | | | | | $Sb_2Te_3$ | | | | | | $(Bi_2Te_3)_{0.25}(Sb_2Te_3)_{0.75}$ | | | | | |
|---|---|---|---|---|---|---|---|---|---|---|---|---|---|---|---|---|---|---|---|---|---|---|---|
| I | 2θ | d(Å) | h | k | l | I | 2θ | d(Å) | h | k | l | I | 2θ | d(Å) | h | k | l | I | 2θ | d(Å) | h | k | l |
| 10 | 17.738 | 5.00 | 0 | 0 | 6 | - | - | - | - | - | - | 4 | 17.44 | 5.080 | 0 | 0 | 6 | 40 | 17.6 | - | 0 | 0 | 6 |
| 100 | 27.616 | 3.23 | 0 | 1 | 5 | 100 | 28.036 | 3.18 | 0 | 1 | 5 | 100 | 28.244 | 3.157 | 0 | 1 | 5 | 100 | 28.1 | - | 0 | 1 | 5 |
| 70 | 38.131 | 2.36 | 1 | 0 | 10 | 100 | 38.10 | 2.36 | 1 | 0 | 10 | 35 | 38.285 | 2.349 | 1 | 0 | 10 | 50 | 38.2 | - | 1 | 0 | 10 |
| 50 | 40.831 | 2.210 | 1 | 1 | 0 | 38 | 42.194 | 2.14 | 1 | 1 | 0 | 6 | 40.700 | 2.215 | 0 | 1 | 11 | 28 | 42 | - | 1 | 1 | 0 |
| | | | | | | | | | | | | 25 | 42.401 | 2.130 | 1 | 1 | 0 | | | | | | |
| 30 | 45.439 | 1.996 | 0 | 0 | 15 | 63 | 44.599 | 2.03 | 0 | 0 | 15 | 4 | 44.599 | 2.030 | 0 | 0 | 15 | 65 | 44.8 | - | 0 | 0 | 15 |
| 30 | 50.032 | 1.823 | 2 | 0 | 5 | 63 | 51.438 | 1.775 | 2 | 0 | 5 | 2 | 50.553 | 1.804 | 1 | 1 | 9 | 22 | 51.6 | - | 2 | 0 | 5 |
| 5 | 54.805 | 1.675 | 1 | 0 | 16 | 63 | 54.058 | 1.695 | 0 | 0 | 18 | 2 | 54.162 | 1.692 | 0 | 0 | 18 | 30 | 54.1 | - | 0 | 0 | 18 |
| 20 | 57.256 | 1.609 | 0 | 2 | 10 | 63 | 58.154 | 1.585 | 0 | 2 | 10 | 8 | 58.436 | 1.578 | 0 | 2 | 10 | 18 | 58 | - | 0 | 2 | 10 |
| 30 | 62.454 | 1.487 | 1 | 1 | 15 | 63 | 63.106 | 1.472 | 1 | 0 | 19 | 8 | 63.202 | 1.470 | 1 | 0 | 19 | 20 | 63 | - | 1 | 0 | 19 |
| 40 | 66.553 | 1.405 | 1 | 2 | 5 | 63 | 66.333 | 1.408 | 0 | 1 | 20 | 2 | 66.333 | 1.408 | 0 | 1 | 20 | 20 | 66.2 | - | 0 | 1 | 20 |

Full Paper

have been employed for analyzing. The TE properties of the crystal were measured along the growth axis at room temperature. Specimens with dimensions 25mm length and 8mm diameter were cut from the ingot for the measurements of electrical conductivity σ, Seebeck coefficient α, and thermal conductivity K. To measure the Seebeck coefficient α, special configuration was designed[23]. The technique based on applying heat to one end of the specimen, measuring the temperature gradient by a Al-Ni and Al-Cr(Alumel-Chromel) thermocouples, and the potential gradient at a 10mm define length of the sample. The seebeck coefficient(α) of the ingot was determined from=ΔV/ΔT.

The electrical conductivity σ was determined by applying current along the length of the sample. From the formula of σ=Il/VA electrical conductivity can be calculated where I is the current, V potential different between two ends of length *l* on the sample, *l* is a defined length and A is the cross section of the sample. Repeated measurements were made rapidly with duration shorter than 1s to prevent errors due to the Peltier and Joule effects. The thermal conductivity K, was measured by same methods as[24].

Having these measurements the figure of merit(Z) at the room temperature was evaluated by the formula $Z=\alpha^2\sigma/K$.

## RESULTS AND DISCUSSION

The preferred orientations of the grains in the crystals were studied by XRD analysis. Figure 2 shows the XRD patterns obtained from powder of the samples. The structure of$(Bi_2Te_3)_{0.25}(Sb_2Te_3)_{0.75}$ is just matched with the $Bi_2Te_3$ '$Sb_2Te_3$ and $Sb_{0.405}Te_{0.595}$,cf. TABLE.

The bars(lower part of the XRD pattern in figure 2 are characteristic lines of planes for $Bi_2Te_3$, $Sb_{0.405}Te_{0.595}$ and $Sb_2Te_3$, structures and unit cells of the compounds. From data sheet of XRD system the intensity of(015), (1010),(110),(0015) and(0210) planes attributed to $Bi_2Te_3$, $Sb_2Te_3$ and, to the unstoiciometric solution of antimony telluride($Sb_{0.405}Te_{0.595}$ solid solutions). The compound is formed by substitution of Sb atoms by the Bi sites of the $Bi_2Te_3$ structure or vice versa. $Sb_{0.405}Te_{0.595}$ solid solution results in anisotropy owing to unstoiciometric correspond to lack of enough Te in the compound. This is due to low vapor point of Te relative to Bi and Sb. The(006) plane is attributed to $Bi_2Te_3$ and $Sb_2Te_3$, and finally(0018) and(1019) planes are related to $Sb_{0.405}Te_{0.595}$ and $Sb_2Te_3$.

**TABLE 2 : Summarized TE properties of the$(Bi_{0.25}Sb_{0.75})_2Te_3$ ingot**

| Parameter | Present work | Ref [27] | Ref [25] | Ref [26] |
|---|---|---|---|---|
| α(μVK$^{-1}$) | 222 | 216.45 | 227 | 215.5 |
| σ(×10$^{-3}$Ω.m)$^{-1}$ | 1205 | 1488 | 512 | 621 |
| K(W/Km) | 2.2 | 2.58 | 1.73 | 1.18 |
| Z(×10$^{-3}$K$^{-1}$) | 2.7 | 2.7 | 1.53 | 2.44 |

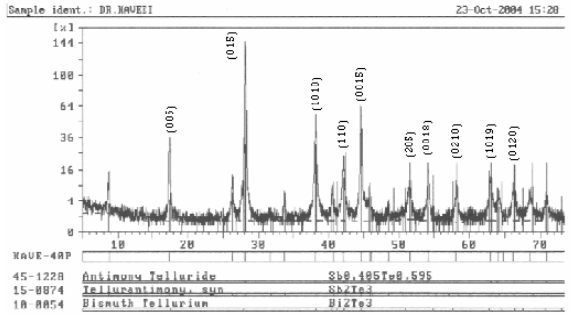


**Figure 2 : XRD pattern obtained from powder of(a) Bi2Te3,(b) p-type$(Bi_{0.25}Sb_{0.75})_2Te_3$**

There were reported[20-21] that, the p-type$(Bi_{0.25}Sb_{0.75})_2Te_3$ compounds were highly dense and flaky. It is there fore, to investigate the preferred orientation of the grains, XRD analyses acquired from the powder of the compound. The XRD analysis showed that, the intensity of the(1015) and(0018) planes are much stronger and attributed to $Bi_2Te_3$ and $Sb_2Te_3$ . In addition, the intensity of(005) and(006) planes have same status.

TABLE 2 summarizes data of the TE properties for the ingot. The measured values of the Seebeck coefficient α, thermal conductivity K and electrical conductivity σ compared with those obtained by[25-27]. In the previous work[27] it was deduced that there may be errors on measurements. However, the XRD characterization was repeated and measurements was carried out with high precision but there were no deviation on the Z value. The relationship between the seebeck coefficient α and the carrier concentration n at a given temperature can be expressed as follow: When electron transport occurs via a conduction band(CB), the seebeck coefficient is defined as[28-29].

$$\alpha = -\frac{k}{e}\left(\ln\frac{N_c}{n}\right) + A$$

where $N_c$ is the effective density of states in the conduction band. The transport or scattering factor A in conduction band depends on the scattering mechanism.

The transport factor A for the CB model depends on the scattering mechanism, and usually ranges between 1 and 3. The dislocations formed during the crystallization decreases the carrier concentration because of the Te vacancy, which is generated by nonbasal slip due to mechanical deformation acts as donor[30-31]. The electrical conductivity σ can be expressed by the following relationship:

$$\sigma = \mu n_c e$$

where e is the electron charge and μ is the carrier mobility. This assumption, may explain the disagreement of our data and corresponding data from the references [20-21] could originate from the fact that with different fractions of the compounds in solid solutions, although the carrier concentration is decreased, the carrier mobility is significantly increased due to the decrease in structural defects. The thermal conductivity, K, slightly decreased probably because of the increase in phonon-grain boundary scattering due to the grain refinement, and then because of annealing partial grain growth due to the recovery. The calculated figure of merit is given in TABLE 2.

## CONCLUSION

p-type$(Bi_{0.25}Sb_{0.75})_2Te_3$ compound was fabricated, and $Z=2.7\times10^{-3}K^{-1}$ has been obtained. The compound has a highest figure of merit compared with recent works. Nevertheless, fractions of Bi and Sb have been examined, The$(Bi_{0.25}Sb_{0.75})_2Te_3$ has highest figure of merit among them. The discrepancies of the measured values of this work and the previous wok are attributed to the measurements on different position on the ingot. There are reports that the stoichiometry of the compound changes along the ingot if along the ingot the zone melting method is employed for crystallization.

## REFERENCES


[1] V.A.Kulbachinski, S.Kawasaki; Phys Status Solidi, **B229(3)**, 1467 **(2002)**.
[2] D.M.Rowe, C.M.Bhandari; Modern thermoelectrics, Holt, Rinehart, and Inston, London, 103 **(1983)**.
[3] C.F.Desai, P.H.Soni, S.R.Bhavsar; Bull.Mater Sci., **22**, 21-3 **(1999)**.
[4] N.B.Brandt, L.G.Lyubutina; Sov.Phys.JETP, **26**, 93 **(1968)**.
[5] B.G.Martin, L.S.Lerner; Phys.Rev., **B68**, 3032 **(1972)**.
[6] T.S.Oh, B.D.Hyun; Kolomoets, Scripta Mater, **42**, 849-854 **(2000)**.
[7] M.P.Volotskii, B.T.Syibnev; Sov.Phys.Semicon., **8**, 682 **(1974)**.
[8] A.S.Okhotin et al.; Thermoelectric generators, Moscow, Atomizdat, in Russian, 32 **(1971)**.
[9] D.M.Rowe; MTS Journal, **27(3)**, 43-48, **(1997)**.
[10] G.S.Nolas, G.A.Slack; American Scientist, **89**, 136, **(2001)**.
[11] G.D.Mahan, H.Ehrenreich, F.Spaepen (Eds.); Solid State Physics, Academic Press, New York, 81 **(1997)**.
[12] F.J.Disalvo; Science, **285**, 703 **(1999)**.
[13] W.E.Bies, R.J.Radtke; Phys.Rev., **B65**, 085208 **(2002)**.
[14] S.J.Youn, A.J.Freeman; Phys.Rev., **B63**, 085112 **(2001)**.
[15] L.I.Anatychuk; 'The Physics of Thermoelectricity', Academy of Science of Ukraine, Institute of thermoelectricity, Kiev, **(1998)**.
[16] M.M.Yim, F.D.Rosi; Sol.Stat.Elec., **15**, 1121 **(1972)**.
[17] A.Yang, F.D.Shephed; J.Electrochem.Soc., **10**8, 197 **(1961)**.
[18] M.M.Ibrahim; Mahmood, Powder Met.Int., **20**, 21 **(1988)**.
[19] D.M.Rowe, U.S.Shukla; Nature, **290**, 765 **(1981)**.
[20] J.Seo, C.Lee; Mater.Sc.Eng., **B49**, 247 **(1997)**.
[21] J.Seo, K.Park; J.Mater.Sci.Lett., **16**, 1153 **(1997)**.
[22] J.O.Sofo; Appl.Phys.Lett., **65**, 2690 **(1994)**.
[23] C.Wood, D.Zoltan; Rev.Sci.Instram, **59(6)**, 951-954 **(1988)**.
[24] R.Taylor; CRC hand book of thermoelectric Ed. M.D.Rowe, CRC Press Boca Raton FL, 165 **(1995)**.
[25] H.Scherrer, S.Scherrer; CRC hand book of thermoelectric Ed. M.D.Rowe, CRC Press Boca Raton FL, 211 **(1995)**.
[26] J.Seo, K.Park; Mater.Res.Bull., **35**, 835 **(2000)**.
[27] G.Kavei, A.A.Khashachi; Journal of thermoelectricity, **3**, 40-45 **(2005)**.
[28] P.A.Cox; Transition Metal Oxides, Oxford University Press, New York, **(1992)**.
[29] T.Kolodiazhnyi, J.E.Greedan; Phys.Rev., **B68**, 085205 **(2003)**.
[30] H.S.Shin, H.P.Ha; J.Phys.Chem.Solids, **58**, 671 **(1997)**.
[31] J.M.Schultz, J.P.Mchugh; J.Appl.Phys., **33**, 2443 **(1962)**.